HHS Public Access

Author manuscript

Anat Rec (Hoboken). Author manuscript; available in PMC 2015 April 07.

Published in final edited form as:

Anat Rec (Hoboken). 2013 August ; 296(8): 1169–1179. doi:10.1002/ar.22727.

Idiopathic microscopic colitis of rhesus macaques: quantitative assessment of colonic mucosa

Amir Ardeshir[*], **Karen L. Oslund**, **Frank Ventimiglia**, **JoAnn Yee**, **Nicholas W. Lerche**, and **Dallas M. Hyde**

California National Primate Research Center, University of California Davis, Davis, CA, USA

Abstract

Idiopathic chronic diarrhea (ICD) is a common cause of morbidity and mortality among juvenile rhesus macaques. While lesions may be absent at colonoscopy, the histopathologic evaluation of the biopsy specimens is consistent with human macroscopic colitis (MC). In this study, we developed an isotropic uniform random sampling method to evaluate macroscopic and microscopic changes and applied it on proximal ascending colon in monkeys. Colonic tissue and peripheral blood specimens were collected from six MC and six control juvenile macaques at necropsy. Uniform random samples were collected from the colon using punch biopsy tools. The volume of epithelium and lamina propria were estimated in thick (25 μm) sections using point probes and normalized to the area of muscularis mucosae. Our data suggests a significant increase of the *Vs* of the lamina propria (1.9 fold, p=0.02) and epithelium (1.4 fold, p=0.05) in subjects with MC. The average colonic surface mucosa area in the MC monkeys increased 1.4 fold over the controls (p=0.02). The volume of the proximal colon in animals with MC showed a 2.4 fold increase over the non-diarrhea control monkeys (p=0.0001). Cytokine, chemokine, and growth factor levels in peripheral blood were found to be correlated with the volume estimate of the lamina propria and epithelium. We found that ICD in macaques has features which simulates human MC and can be used as a spontaneous animal model for human MC. Furthermore, this developed sampling method can be used for unbiased evaluation of therapeutics in clinical trials of this animal model.

INTRODUCTION

Microscopic colitis in rhesus macaques

Diarrhea is a frequent health problem in rhesus macaque colonies.(Hird et al., 1984; Elmore et al., 1992; Adler et al., 1993; Sestak et al., 2003; Blackwood et al., 2008) The incidence of diarrhea in NHP colonies varies but may involve up to 15–20% of the population annually. *Shigella*, *Campylobacter*, *Yersinia* and *Salmonella* are common causes of diarrhea in these colonies.(Brady and Morton, 1998; Blackwood et al., 2008) However, in a subset of these diarrhea cases no pathogenic bacteria and parasites or other common causes are found and defined as idiopathic chronic diarrhea (ICD). (Broadhurst et al., 2012)

Correspondence to: Amir Ardeshir, California National Primate Research Center, University of California Davis, Davis, CA 95616, USA, Phone: (530) 754-8588, Fax: (530) 752-2880, aardeshir@ucdavis.edu.

At the California National Primate Research Center (CNPRC) approximately 25% of the diarrhea cases are diagnosed as ICD (5% annual incidence). The incidence of ICD cases has been reported as high as 15% of the population in other breeding colonies. The histopathologic analysis of the colonic tissue specimens of ICD cases reveal characteristic changes including lymphocytic/plasmacytic colitis with crypt changes (hyperplasia, goblet cell depletion, crypt abscesses), surface epithelium alterations (attenuation, tufting, exocytosis and micro-ulceration) as well as lamina propria changes (inflammatory cell infiltrates, fibrosis, amyloid deposition). Cecum and proximal ascending colon in the large intestine are typically involved in ICD as evidenced by a marked thickening of the mucosa and possible inflammatory reflux into the terminal ileum.

The endoscopic appearance of the colonic lining is normal (or near normal) however colonic biopsy specimens are characterized by abnormal histopathology.(Pardi et al., 2002; Olesen et al., 2004; Pardi, 2004; Zippi et al., 2010) These features of the ICD cases as well as its clinical complications (watery, non-bloody diarrhea that lasts for over a month period) are similar to those found in human microscopic colitis (MC), a subtype of human inflammatory bowel disease.(Kingham et al., 1982; Bohr et al., 2000; Jaskiewicz et al., 2006)

Quantitative pathology

Morphometry is the measurement of the structures in three dimensions and is often the goal of structural quantitation. Since much of the structural data in normal and pathologically altered tissues requires the use of tissue sections, stereology must be used.(Elias and Hyde, 1980) Stereology is a well-defined set of techniques that provides quantitative information about three dimensional structures obtained from lower dimensions, e.g. from two dimensional sections.(Elias and Hyde, 1980; Gundersen et al., 1988; Hyde et al., 1992) Stereology is used to estimate multiple structural parameters such as number of cells, length, surface area, and volume, in tissue and provides objective information about the third dimension.(Hyde et al., 2007) The prerequisite for any stereological method is an accurate, unbiased sampling of the organ of interest.(Gundersen and Jensen, 1987; Gundersen et al., 1988; West and Gundersen, 1990; Hyde et al., 1992; Gundersen et al., 1999; Cruz-Orive and Gual-Arnau, 2002) This unbiased tissue sampling may require more time but, but can be stored in digital image format and used for estimations of structural features to answer a variety of questions even if stored in digital image format. (Hyde et al., 1991; Hyde et al., 1992)

MATERIALS AND METHODS

Animal Selection

Twelve Juvenile rhesus macaques, aged nine months to four years (Table 1), with a history of ICD were randomly selected. Control subjects were selected randomly from a list of non-diarrhea animals sent to necropsy for a variety of medical reasons, primarily trauma. Monkeys with at least one out of their last three stool examinations positive for ova, *parasites*, *Salmonella*, *Shigella*, *Campylobacter*, or *Yersinia* were excluded from the study pool. Likewise, subjects with a positive immunofluorescence assay (IFA) for *Giardia spp. and Cryptosporidium spp.* as well as those with other obvious causes of diarrhea were

excluded from the study. All animals were identified as *Simian immunodeficiency virus* and *Simian betaretrovirus* free.

Estimation of organ volume and luminal surface

The volume estimation of the entire organ enables morphologic changes to be quantified within the whole organ. The Cavalieri estimator is a simple, well known technique in volume estimation. For parenchymal organs such as lung, liver, and kidney, it involves cutting the organ into slabs of equal thickness and determining the cumulative area by point counting the organ surface and multiplying by the average slab thickness.(Luciw et al., 2011) It is a very efficient estimator of volume.(Hyde et al., 1992) Performing a Cavalieri estimate on hollow organs such as the gastrointestinal tract does not require sectioning the organ into slabs. Rather, the opened organ can be photographed with a ruler in place and an average tissue thickness measured with calipers. Point counting from a grid composed of countable points with a known area per point overlying the digital image determines the surface area which is multiplied by the average tissue thickness to estimate volume.

Organ sample collection

The concept of unbiased sampling requires that each part of an organ of interest has been randomly selected and has an equal chance of being selected for analysis. This requirement is best met by introducing randomness into the sampling process and using efficient systematic uniform random sampling (SURS).(Braendgaard et al., 1990; Larsen, 1998) This technique has been used extensively in stereological analysis and was the basis of our sample selection at the gross and histologic level. Practical application of SURS required the selection of a random number from a random number table. Then starting with the random number, samples were collected at a set sampling interval throughout the tissue.(Gundersen and Jensen, 1987; Braendgaard et al., 1990; Wreford, 1995; Luciw et al., 2011) SURS ensures that every point in the tissue has an equal chance of being selected for analysis. To start the sampling, the whole colon was collected at the necropsy and cut into three sections (Figure 1A). The colonic tubular structure was opened (Figures 1B, 1C). Opened colonic tissues were fixed overnight in 10% buffered formalin (figure 1D). The ultimate goal was to collect approximately 10 unbiased samples from the proximal colon which could be embedded in paraffin blocks. A Plexiglas® grid template containing evenly spaced 5 mm holes spaced at a known interval was randomly placed over the tissue. Using a random start, tissue underlying the holes, was sampled at a set interval using a 5-mm biopsy punch colonic (Figures 1E, 1F). The holes that partially covered at least 50% of the colon were sampled. Punch biopsies were cut in half (Figure 1G) and were placed in cassettes on their cut surface and embedded in paraffin (Figure 1H). Paraffin embedded tissues were cut (25 μm) and stained with hematoxylin and eosin (H&E). Digital images, 25 μm deep with a stack of 15 images at 1.67 μm intervals, were acquired with an automated slide scanner (Olympus VS110 whole slide scanner) for storage in a database (Figure 1I). With a guard region of one image plane on the top and at the bottom the total depth of tissue used for analysis was 21.66 μm.(West et al., 1991; Garman et al., 2001; Uranova et al., 2004) Six middle image planes out of total 13 were used for quantitation.

Stereology

Different probes were applied to microscopic sections to quantify the structural features, and the intersection of the probe and the feature of interest was counted.(Hsia et al., 2010b) Point hits were used to estimate volume, and line (Fakir probes) intersections were used for estimation of the surface area. In stereology, the measurements are commonly treated with the calculation of ratios (i.e. quantity of structure per unit volume of reference compartment). It is essential that the reference structure and the structure of interest be measured at the same time and that the reference space not significantly change between individuals.(Gundersen et al., 1988; Amann et al., 1992; Hsia et al., 2010a) Stereological methods for the estimates are well established and there are several software programs available to assist in systematic uniform random sampling (URS) of microscopic fields for analysis and application of probes on the selected fields. We used Visiopharm™ MicroImager and NewCast to perform the URS.

The following is a brief overview of approaches for structural estimates:

Estimation of volume density—The volume density of the compartment of interest in the organ is the sum of the points hitting the compartment of interest divided by the sum of the points hitting the reference (Table 2):

$$Vv(Y,r)=\frac{\sum_{i=1}^{n} P(Y)i}{\sum_{i=1}^{n} P(ref)i}$$

where *n* is the number of the fields of view, *P(Y)* is the numbers of points hitting the compartment of interest (epithelium or lamina propria of the proximal colon), and *P(ref)* is the numbers of point hitting the colonic mucosa (reference volume).

Surface density—Surface estimation requires linear probes (Table 2). Intersections between line probes and the feature of interest are countable events. Specialized isotropic fakir probes, a module of the ELLIPSE® software package (version 2.0.8.1, ELLIPSE®, Kosice, Slovakia) were used to offset the bias of the tissue orientation at the time of collection (i.e. biopsies were all embedded in the same orientation). The fakir probes were randomly oriented in 3-dimentions, thereby accounting for tissue orientation bias. (Kubinova, 1998; Kubinova and Janacek, 1998, 2001; Kubinova et al., 2001; Kubinova et al., 2003; Janacek et al., 2011)

Surface density, S_v, is defined as:

$$Sv(Y,r)=\frac{2.\sum_{i=1}^{n} Ii}{l/p \cdot \sum_{i=1}^{n} P(ref)i}$$

where *n* is the number of the fields of view, *Ii* is the number of intersections of the feature of interest (muscularis mucosae) with the linear probe, *l/p* is the length of the line probe per grid point, and *P(ref)* is the number of points hitting the colonic mucosa (reference volume).

Volume /surface estimation—All the counts were performed using the same image field of view (magnification and image field size) for each sample from the proximal colon; to normalize the volume count values, a volume/surface estimation was calculated for the volume of each compartment (lamina propria and epithelium), where the estimated surface used came from muscularis mucosae. Crypt and the surface epithelium were considered as epithelium. Lamina propria was measured as the thin layer of cellular infiltrations which lies beneath the epithelium and the muscularis mucosae.

$$\frac{Vv(Y,r)}{Sv(Y,r)}=\frac{l/p\cdot\sum_{i=1}^{n}P(ref)i}{2\cdot\sum_{i=1}^{n}Ii}\div\frac{\sum_{i=1}^{n}P(ref)i}{\sum_{i=1}^{n}P(Y)i}$$

or

$$\frac{Vv(Y,r)}{Sv(Y,r)}=\frac{l/p\cdot\sum_{i=1}^{n}P(ref)i}{2\cdot\sum_{i=1}^{n}Ii}\times\frac{\sum_{i=1}^{n}P(Y)i}{\sum_{i=1}^{n}P(ref)i}$$

When the same field of view is used to count the reference space for both the volume and surface estimates the value is identical for both and divide to one in the equation. So, *Vv(Y,r)/Sv(Y,r)* can be simplified as:

$$Vs(Y,r)=\frac{Vv(Y,r)}{Sv(Y,r)}=\frac{l/p\cdot\sum_{i=1}^{n}P(Y)i}{2.\sum_{i=1}^{n}Ii}$$

The simplified calculation reduces the time of the feature counting due to omitting the *P(ref)*, where *n* is the number of the fields of view, *Ii* is the number of intersections of the feature of interest (muscularis mucosae) with the linear probe, *l/p* is the length of the line per grid point (density in measurable units), and *P(Y)* is the numbers of points hitting the epithelium and lamina propria.

Tissue shrinkage—A juvenile non-diarrhea and a MC macaques were selected age matched with the study cohort animals. Fresh colonic tissue samples (proximal section) were collected and the width and length were measured at the necropsy and seven days post fixation. Punch biopsy tool was used to cut the tissues samples and the diameter of the punches was measured before and after embedding in the paraffin. The shrinkage percentage in each step was calculated and used to determine the total shrinkage. The total shrinkage (in percentage) was calculated as the product of two steps shrinkage numbers multiplied by 100.

The Volume /surface estimation for each compartment was divided by the total shrinkage to adjust for the shrinkage factor. *Vs* presented in this manuscript is adjusted for shrinkage. (Dorph-Petersen et al., 2001)

Multiplex analyses of inflammatory mediators in peripheral blood

Cytokine, chemokine, and growth factor levels were measured using commercially available xMAP® (Luminex Corporation, Austin, TX) technology based microbead immunoassay reagents from Life Technologies (Carlsbad, CA). The assay is formatted to simultaneously detect and quantitate levels of 28 monkey specific analytes. The cytokines used in this assay were IL-1b, IL-1RA, IL-2, IL-4, IL-5, IL-6, IL-10, IL12, IL-15, IL-17, G-CSF, CM-CSF, IFN-γ, and TNF-α. The chemokines were eotaxin, IL-8, MCP-1, MDC, MIF, MIG, MIP-1a, MIP-1b, I-TAC, and RANTES. The growth factors were EGF, FGF-basic, HGF, and VEGF. In these solid phase sandwich immunoassays, microbeads of defined spectral properties coated with analyte specific antibodies were incubated with serum samples to capture the specific analytes. After washing, the beads were then reacted with analyte-specific biotinylated detector antibodies that bound to the appropriate immobilized analytes. After additional washing, the beads were reacted with streptavidin-R-phycoerythrin that bound to the biotinylated detector antibodies associated with the immune complexes on the beads, forming a four-member solid phase sandwich. After a final washing to remove all unbound material, the beads were analyzed in a Luminex instrument. By monitoring the spectral properties of the beads and amount of associated R-phycoerythrin fluorescence for each serum sample and comparing to known standards, the concentration of each analyte was determined.(Teigler et al., 2012)

RESULTS

Sampling method

Our goal in sampling of the colon was to collect isotropic uniform random (IUR) samples. However, the texture of the colonic tissues does not have the rigidity of some the parenchymal organs such as kidney, or even lung. It is difficult to randomly position the tissue even after it is fixed. One way to fix the anisotropy of the punch biopsy samples would be to use the Isector, which is a small rubber sphere mold that contains 5 mm diameter holes to hold small specimens and subsequently allows rolling in random directions on the table to randomly orient the tissue specimens and provide isotropic sections.(Mayhew, 1992; Nyengaard and Gundersen, 1992; Lokkegaard et al., 2001; Bruel and Nyengaard, 2005; Eisele et al., 2008; Dougherty et al., 2010) Although, this is a relatively easy solution it may be difficult to differentiate epithelium and muscularis mucosae in isotropic sections. Another method that can be applied to the collected samples to resolve anisotropy is based on randomizing the test probe in the appropriate dimension. In the current study we used this technique on the collected samples to produce isotropic test systems. The surface compartment of interest, muscularis mucosae of the colon was used to normalize the volume estimate values (epithelium and lamina propria). Line probes (Table 2) were used to estimate the surface area. The intersections of the lines and the outer edge of the muscularis mucosae in six middle focal planes of the thick colonic sections were recorded (Figure 2). As a general rule, the probe density was adjusted to count at least 200

points in a total of six focal planes (Figure 3) from at least 10 punch biopsy sections.(Cruz-Orive and Weibel, 1990) This helped the sampler to collect randomly distributed tissue samples. The duration of each sampling was recorded (at the time of start of the procedure to the time of capping the collection tubes). The process time ranged from an hour to an hour and a half, depending on the size and disease status of the animal. Our data suggests that animals with MC require less time to collect the samples ($p<0.05$) (Figure 3) due to fact that almost no fecal matter was seen in the colon thus requiring almost no cleaning. In contrast, control animals (animals with no diarrhea at the time of sample collection) usually have impacted proximal ascending and transverse colon. Also, our data demonstrates that older animals require more time to collect the samples due to the increased size of the colon.

The surface area of the proximal colonic segment was calculated using the recorded length and the average of the width of the two ends (proximal and distal). The data suggested that the average surface area in the MC monkeys increased 1.4 fold over the control animals ($p=0.02$) (Figure 4). We also estimated the volume of the colonic compartment using the recorded length, average width, and the height of the segment at the time sampling. Data indicates that the volume of the proximal colon in animals with MC has a 2.4 fold increase over the control monkeys (non-diarrhea) cases ($p=0.0001$) (Figure 5).

Stereological analysis

Thick (25μm) proximal ascending colonic sections were optically dissected and the six middle sections were used to count the colonic mucosa features. We used the muscularis mucosae to normalize the volume estimates. The estimated *Vv* of the features of interest (epithelium and lamina propria) was normalized to the estimated *Sv* of the muscularis mucosae. The *V/S* (mm^3/mm^2) estimate was corrected for shrinkage. The total one dimensional shrinkage (the product of post fixation- and post embedding-shrinkage) was calculated as 76.81% in normal colon and 74.49% in colon with MC. The results suggest an average increase in this ratio for both compartments in MC animals compared to control animals. The average fold increase for *Vs* of epithelium and lamina propria was estimated 1.4 and 1.9 respectively. Data suggested a marginally significant increase of the *Vs* of the surface epithelium ($p=0.05$) and a statistically significant increase of the *Vs* of the lamina propria in subjects with MC ($p=0.02$) (Figure 7).

Coefficient of error and coefficient of variation

The coefficient of variation and coefficient of error (CE) of the *Vs* of epithelium and lamina propria were calculated as the ratio of standard variation or standard error of the mean of *Vs* estimates divided by the mean *Vs* estimates. (Table 3). The relatively small CE (<0.2) suggests that the effort put into the sampling cascade (tissue blocks per individual, percentage of sampling area of each block) provided a precise estimate of the *Vs* per compartment of interest.(Weibel et al., 2007)

Serologic assay

Foreground fluorescence intensities were subtracted from background (ΔΔFI) and the values less than the minimum estimated concentration were treated as zeros. No analytes were detected for nine cytokines (GM-CSF, IL-2, IL-5, IL-6, IL-10, IL-15, IL-17), one chemokine

(I-TAC) and one growth factor (VEGF). Peripheral blood pro-inflammatory cytokines were detected at higher levels in MC as compared to controls. The average values of serum INF-γ, TNF-α, IL-8 and IL-12 were elevated in monkeys with MC. The average INF-γ value increased two fold (p=0.009), TNF-α 1.4 fold (p=0.004), IL-8 2.9 fold (p=0.021) and IL-12 2.4 fold (p=0.012) demonstrating an inflammatory response in the peripheral blood (figure 8). Chemokine were detected at higher levels for MIG, with average increase of 1.5 (p=0.030) and lower MIF (p=0.048) for MC subjects as compared with controls. No significant differences were found in several cytokines (G-CSF, IL-1b, IL-1RA, IL-4), chemokines (eotaxin, MCP-1, MDC, MIP-1a, MIP-1b, RANTES) as well as growth factors (Eotaxin, MCP-1, MDC, MIP-1a, MIP-1b, RANTES) between the two groups. The R square values were calculated using the square of the sample correlation coefficient and were analyzed to describe the relative amount of variance of the *Vs* differences for colonic compartments (epithelium and lamina propria) as explained or accounted for by the serum analytes. Circulatory MIG (p=0.01) and IL-1β (p=0.028) were correlated with the volume estimates of the proximal colon (Table 4). A positive correlation between the lamina propria volume estimates (*Vs*) and values for circulatory INF-γ (p=0.042), IL-1β (p=0.020), TNF-α (p=0.021) and MIG (p=0.004) were found (Table 4).

DISCUSSION

MC is a chronic non-bloody diarrhea which accounts for about 10% of chronic diarrhea in humans.(Fernandez-Banares et al., 1999; Fine and Seidel, 2000; Shah et al., 2001; Pardi et al., 2002; Pardi et al., 2007) MC is a less commonly reported form of human inflammatory bowel disease (IBD). The two major forms of human IBD are lymphocytic colitis and collagenous colitis.(Fernandez-Banares et al., 1999; Fine et al., 2000; Shah et al., 2001; Olesen et al., 2004; Pardi, 2004; Limsui et al., 2009) It has been suggested that the prevalence of MC is underestimated and the true prevalence of this disease is increasing in humans.(Olesen et al., 2004; Limsui et al., 2009; Zippi et al., 2010; Yen and Pardi, 2011) The cause(s) is uncertain (Pardi et al., 2007) but it has been suggested that infectious agents or some drugs may trigger the problem.(Pardi et al., 2002; Olesen et al., 2004; Beaugerie and Pardi, 2005; Fernandez-Banares et al., 2007)

In rhesus macaques, idiopathic chronic diarrhea (ICD) is a common cause of morbidity and mortality among juvenile animals.(Hird et al., 1984; Adler et al., 1993; Sestak et al., 2003; Fox et al., 2007; Blackwood et al., 2008; McKenna et al., 2008) This condition is characterized histologically as colitis with distinct plasmacytic and lymphocytic infiltrates. The clinical diagnosis consists of multiple negative cultures for common pathogens, as well as no pathogenic parasite. Broad spectrum antibiotic therapy as well as anti-parasitic therapy is usually part of the workup for these cases. While no lesions may be seen at the time of total colonoscopy, the histopathologic evaluation demonstrates crypt changes (hyperplasia, goblet cell depletion, crypt abscesses), surface epithelial changes (attenuation, tufting, exocytosis and micro-ulceration) and expansion of the lamina propria (inflammatory cell infiltrates, fibrosis, and occasional amyloid deposition).(Hird et al., 1984; Adler et al., 1993; Blackwood et al., 2008; Wilk et al., 2008) The disease primarily involves the cecum and proximal ascending colon with a marked thickening of the mucosa and may involve inflammatory reflux into the terminal ileum. Colonic lymph nodes are usually enlarged. In

more severe cases, the inflammation can extend from the proximal ascending colon to more distal regions or even the rectum.

Clinically these monkeys show watery, non-bloody diarrhea that leads to weight loss, dehydration, and no response to common therapies and will ultimately need to be euthanized for ethical considerations. In breeding colonies of the rhesus macaques this condition is a common cause for euthanasia among juvenile macaques and accounts for about half of the medical culls which are not related to research. Although several viral and bacterial agents have been associated with this syndrome, no published study was found to support the causal relationship between these agents and the pathophysiology of MC in macaques. (Duhamel et al., 1997; Fox et al., 2001; Fox et al., 2007; Farkas et al., 2012). It has been suggested that animals reared in a nursery and male monkeys are more likely than breast-fed and female monkeys to develop this condition.(Elmore et al., 1992)

In the current study, we applied stereological techniques to collect samples and to quantitatively and unbiasedly evaluate the histopathologic changes in the colon of MC animals compared to control macaques. In the process of sampling we used a plastic template to collect the samples in a stratified random manner. Although stratified random sampling method has been used extensively in parenchymal organs (lung lobes, liver lobes, heart, brain, kidney), colon is not amenable to standard sampling techniques. The hollow, non-rigid structure of the colon makes the process of sampling challenging because sampling is only feasible in a transmural orientation. Thus, we used punch biopsies from the mucosa through the smooth muscle wall creating a biased sample orientation. We employed randomized linear probes (“fakir probes”) in the reference space to overcome this sampling bias.

Another possible method to unbiasedly sample colon would be to fix the colon in its natural tubular state filled with agar, and using a random start to cut and perform the sampling. This potentially would save time and resources. In some tissue sections with a distinct vertical axis thick vertical sections probed with cyloids or sine-weighted probes may be the easiest method to address the orientation. (Gundersen et al., 1988; West, 2013) Unfortunately, due to specific characteristics of the colonic biopsy tissues these methods were not applicable here. Small colonic punch biopsies curl up after fixation and make it almost impossible to orient the tissues correctly. Alternatively, due to the small size of the tissue blocks, isector molds (Nyengaard and Gundersen, 1992) could be a practical method in this study. Isectors are small rubber molds with spherical cavities that can be used for small specimens embedding. Rolling the embedded tissue in a sphere randomly on the bench top provides the isotropy.

Using a slide scanner to scan a 15 stack of images was tremendously helpful to decrease the amount of time. The relatively large number of stacks of high resolution images provided a great amount of flexibility in choosing the guard region but on the other hand required great amount of disc storage. The high resolution quality may not be critical when estimating the larger tissue compartments (such as surface epithelium or lamina propria) however may act as an imperative step in the process, when the cell types or smaller compartments is of an interest.

To estimate the macroscopic volume of the proximal colon the length and width (proximal and distal) were measured. The average width, length and the average thickness (measured at multiple locations using calipers) were used to estimate the volume. Alternatively, the volume displacement or buoyant weight of the organ and assuming a specific gravity of one could be used. But due to the attachment of the stool particles to the surface we preferred using the direct measurement technique.

Our data demonstrates that the macroscopic volume of the colon in MC cases was increased 2.5 fold over controls (p=0.0001) accounted for by an increase in the average *Vs* of lamina propria (p=0.02) and increase in the epithelium *Vs* compartments (crypt and the surface epithelium) (p=0.05) (Figure 7). The increase in volume in the lamina propria is likely due to a significant inflammatory reaction possibly associated with some fibrosis. The increase in the epithelial compartment is likely secondary to a hyperplastic epithelial response associated with the inflammatory reaction (i.e. crypt hyperplasia). Goblet cell hyperplasia could also be a contributing factor as these cells are larger than most enterocytes. These results were supported by the observed microscopic changes and compartment estimations. The volume of the colonic compartments (epithelium and lamina propria) was normalized to the estimated surface of the muscularis mucosae. The estimated *Vv/Sv* (*Vs*) was also adjusted for the tissue shrinkage throughout the process of fixation and tissue embedding in paraffin. Further studies are necessary to characterize the subcomponents of the lamina propria and epithelium and to investigate cellular changes that account for the increase volume of these microenvironments.

The circulatory cytokine and chemokine profile was correlated with the stereological estimates (*Vs*) of the epithelium and lamina propria (Figures 11, 12, Table 4). Although this correlation may be used in therapeutic response evaluation and the progress of the inflammatory changes, more subjects are needed to assess this association.

Overall, features of ICD mimic MC (specifically lymphocytic colitis) in humans. Clinical symptoms (watery, non-bloody diarrhea for more than a month), colonic endoscopy appearance (normal colonic mucosa or with minimal changes), and histopathologic analysis of the colonic samples (lymphocystes and plasma cells infiltrates in lamina propria) with damaged surface epithelium (damage to surface epithelium, attenuation, tufting, exocytosis and micro-ulceration of epithelial cells and sometimes detachment) are seen in macaques with ICD. It also has been suggested that intraepithelial lymphocytes in the colonic mucosa are increased in lymphocytic form of microscopic in human patients.(Kingham et al., 1982; Fernandez-Banares et al., 1999; Fraser et al., 2002; Pardi et al., 2002; Warren et al., 2002; Abdo et al., 2003; Olesen et al., 2004; Pardi, 2004; Brown and Lambie, 2008; Tangri and Chande, 2009; Zippi et al., 2010; Fernandez-Banares et al., 2011) This needs to be investigated to better characterize the inflammation.

ACKNOWLEDGEMENT

Authors would like to thank CNPRC Pathology Unit and Clinical Laboratories.

Funding

This publication was made possible by Grant Number P51 OD011107 from the Office of the Director (OD), a component of the National Institutes of Health (NIH), and NIH Roadmap for Medical Research. Its contents are solely the responsibility of the authors and do not necessarily represent the official view of OD or NIH. Information on OD is available at http://www.nih.gov/icd/od/.

REFERENCES

Abdo AA, Urbanski SJ, Beck PL. Lymphocytic and collagenous colitis: the emerging entity of microscopic colitis. An update on pathophysiology, diagnosis and management. Canadian journal of gastroenterology = Journal canadien de gastroenterologie. 2003; 17:425–432. [PubMed: 12915915]

Adler, RR.; Moor, PF.; Schmucker, DL.; Lowenstine, LJ. Chronic Colitis, Juvenile. In: Jones, TC.; Mohr, U.; Hunt, RD., editors. Macaca mulatta. Nonhuman primates. New York, NY: Springer-Verlag.; 1993. p. 81-87.

Amann K, Wiest G, Zimmer G, Gretz N, Ritz E, Mall G. Reduced capillary density in the myocardium of uremic rats--a stereological study. Kidney international. 1992; 42:1079–1085. [PubMed: 1453595]

Beaugerie L, Pardi DS. Review article: drug-induced microscopic colitis - proposal for a scoring system and review of the literature. Alimentary pharmacology & therapeutics. 2005; 22:277–284. [PubMed: 16097993]

Blackwood RS, Tarara RP, Christe KL, Spinner A, Lerche NW. Effects of the macrolide drug tylosin on chronic diarrhea in rhesus macaques (Macaca mulatta) . Comparative medicine. 2008; 58:81–87. [PubMed: 19793461]

Bohr J, Olesen M, Tysk C, Jarnerot G. Collagenous and lymphocytic colitis: a clinical and histopathological review. Canadian journal of gastroenterology = Journal canadien de gastroenterologie. 2000; 14:943–947. [PubMed: 11125185]

Brady, A.; Morton, D. Gastrointestinal system: approach to diarrhea diagnosis and treatment. In: Bennett, TB.; Abee, CR.; Henrickson, R., editors. Nonhuman primates in biomedical research: Diseases. San Diego: Academic Press; 1998.

Braendgaard H, Evans SM, Howard CV, Gundersen HJG. The Total Number of Neurons in the Human Neocortex Unbiasedly Estimated Using Optical Disectors. J Microsc-Oxford. 1990; 157:285–304.

Broadhurst MJ, Ardeshir A, Kanwar B, Mirpuri J, Gundra UM, Leung JM, Wiens KE, Vujkovic-Cvijin I, Kim CC, Yarovinsky F, Lerche NW, McCune JM, Loke Pn. Therapeutic Helminth Infection of Macaques with Idiopathic Chronic Diarrhea Alters the Inflammatory Signature and Mucosal Microbiota of the Colon. PLoS pathogens. 2012; 8:e1003000. [PubMed: 23166490]

Brown IS, Lambie DLJ. Microscopic colitis with giant cells: a clinico-pathological review of 11 cases and comparison with microscopic colitis without giant cells. Pathology. 2008; 40:671–675. [PubMed: 18985521]

Bruel A, Nyengaard JR. Design-based stereological estimation of the total number of cardiac myocytes in histological sections. Basic Res Cardiol. 2005; 100:311–319. [PubMed: 15795797]

Cruz-Orive LM, Gual-Arnau X. Precision of circular systematic sampling. Journal of microscopy. 2002; 207:225–242. [PubMed: 12230491]

Cruz-Orive LM, Weibel ER. Recent stereological methods for cell biology: a brief survey. The American journal of physiology. 1990; 258:L148–L156. [PubMed: 2185653]

Dorph-Petersen KA, Nyengaard JR, Gundersen HJ. Tissue shrinkage and unbiased stereological estimation of particle number and size. Journal of microscopy. 2001; 204:232–246. [PubMed: 11903800]

Dougherty RH, Sidhu SS, Raman K, Solon M, Solberg OD, Caughey GH, Woodruff PG, Fahy JV. Accumulation of intraepithelial mast cells with a unique protease phenotype in T(H)2-high asthma. J Allergy Clin Immun. 2010; 125:1046–1053. [PubMed: 20451039]

Duhamel GE, Elder RO, Muniappa N, Mathiesen MR, Wong VJ, Tarara RP. Colonic spirochetal infections in nonhuman primates that were associated with Brachyspira aalborgi, Serpulina pilosicoli, and unclassified flagellated bacteria. Clin Infect Dis. 1997; 25:S186–S188. [PubMed: 9310673]

Eisele JC, Schaefer IM, Nyengaard JR, Post H, Liebetanz D, Brul A, Muhlfeld C. Effect of voluntary exercise on number and volume of cardiomyocytes and their mitochondria in the mouse left ventricle. Basic Res Cardiol. 2008; 103:12–21. [PubMed: 18004633]

Elias H, Hyde DM. An elementary introduction to stereology (quantitative microscopy). The American journal of anatomy. 1980; 159:412–446. [PubMed: 7013463]

Elmore DB, Anderson JH, Hird DW, Sanders KD, Lerche NW. Diarrhea rates and risk factors for developing chronic diarrhea in infant and juvenile rhesus monkeys. Laboratory animal science. 1992; 42:356–359. [PubMed: 1434494]

Farkas T, Falkenstein KP, Bohm RP, Pecotte J, Sestak K. High incidence of rhesus enteric calicivirus infections and diarrhea in captive juvenile macaques: a likely association. Journal of medical primatology. 2012

Fernandez-Banares F, Esteve M, Espinos JC, Rosinach M, Forne M, Salas A, Viver JM. Drug consumption and the risk of microscopic colitis. The American journal of gastroenterology. 2007; 102:324–330. [PubMed: 17100977]

Fernandez-Banares F, Salas A, Esteve M, Pardo L, Casalots J, Forne M, Espinos JC, Loras C, Rosinach M, Viver JM. Evolution of the incidence of collagenous colitis and lymphocytic colitis in Terrassa, Spain: a population-based study. Inflammatory bowel diseases. 2011; 17:1015–1020. [PubMed: 20878755]

Fernandez-Banares F, Salas A, Forne M, Esteve M, Espinos J, Viver JM. Incidence of collagenous and lymphocytic colitis: a 5-year population-based study. The American journal of gastroenterology. 1999; 94:418–423. [PubMed: 10022639]

Fine KD, Seidel RH. The prevalence, anatomic distribution, and diagnosis of colonic causes sf chronic diarrhea. Gastrointest Endosc. 2000; 51:318–326. [PubMed: 10699778]

Fine KD, Seidel RH, Do K. The prevalence, anatomic distribution, and diagnosis of colonic causes of chronic diarrhea. Gastrointest Endosc. 2000; 51:318–326. [PubMed: 10699778]

Fox JG, Boutin SR, Handt LK, Taylor NS, Xu S, Rickman B, Marini RP, Dewhirst FE, Paster BJ, Motzel S, Klein HJ. Isolation and characterization of a novel helicobacter species, "Helicobacter macacae," from rhesus monkeys with and without chronic idiopathic colitis. Journal of clinical microbiology. 2007; 45:4061–4063. [PubMed: 17928421]

Fox JG, Handt L, Xu S, Shen Z, Dewhirst FE, Paster BJ, Dangler CA, Lodge K, Motzel S, Klein H. Novel Helicobacter species isolated from rhesus monkeys with chronic idiopathic colitis. Journal of medical microbiology. 2001; 50:421–429. [PubMed: 11339249]

Fraser AG, Warren BF, Chandrapala R, Jewell DP. Microscopic colitis: a clinical and pathological review. Scand J Gastroentero. 2002; 37:1241–1245.

Garman RH, Fix AS, Jortner BS, Jensen KF, Hardisty JF, Claudio L, Ferenc S. Methods to identify and characterize developmental neurotoxicity for human health risk assessment. II: Neuropathology. Environ Health Persp. 2001; 109:93–100.

Gundersen HJ, Jensen EB. The efficiency of systematic sampling in stereology and its prediction. Journal of microscopy. 1987; 147:229–263. [PubMed: 3430576]

Gundersen HJG, Bendtsen TF, Korbo L, Marcussen N, Moller A, Nielsen K, Nyengaard JR, Pakkenberg B, Sorensen FB, Vesterby A, West MJ. Some New, Simple and Efficient Stereological Methods and Their Use in Pathological Research and Diagnosis - Review Article. Apmis. 1988; 96:379–394. [PubMed: 3288247]

Gundersen HJG, Jensen EBV, Kieu K, Nielsen J. The efficiency of systematic sampling in stereology-reconsidered. J Microsc-Oxford. 1999; 193:199–211.

Hird DW, Anderson JH, Bielitzki JT. Diarrhea in nonhuman primates: a survey of primate colonies for incidence rates and clinical opinion. Laboratory animal science. 1984; 34:465–470. [PubMed: 6513506]

Hsia CC, Hyde DM, Ochs M, Weibel ER. An official research policy statement of the American Thoracic Society/European Respiratory Society: standards for quantitative assessment of lung structure. Am J Respir Crit Care Med. 2010a; 181:394–418. [PubMed: 20130146]

Hsia CCW, Hyde DM, Ochs M, Weibel ER, Quantitat AEJTF. An Official Research Policy Statement of the American Thoracic Society/European Respiratory Society: Standards for Quantitative Assessment of Lung Structure. Am J Resp Crit Care. 2010b; 181:394–418.

Hyde DM, Magliano DJ, Plopper CG. Morphometric Assessment of Pulmonary Toxicity in the Rodent Lung. Toxicol Pathol. 1991; 19:428–446. [PubMed: 1813987]

Hyde DM, Magliano DJ, Reus E, Tyler NK, Nichols S, Tyler WS. Computer-assisted morphometry: point, intersection, and profile counting and three-dimensional reconstruction. Microscopy research and technique. 1992; 21:262–270. [PubMed: 1638048]

Hyde DM, Tyler NK, Plopper CG. Morphometry of the respiratory tract: avoiding the sampling, size, orientation, and reference traps. Toxicol Pathol. 2007; 35:41–48. [PubMed: 17325971]

Janacek J, Cvetko E, Kubinova L, Travnik L, Erzen I. A novel method for evaluation of capillarity in human skeletal muscles from confocal 3D images. Microvascular research. 2011; 81:231–238. [PubMed: 21145900]

Jaskiewicz K, Rzepko R, Adrych K, Smoczynski M. Microscopic colitis in routine colonoscopies. Digestive diseases and sciences. 2006; 51:241–244. [PubMed: 16534662]

Kingham JG, Levison DA, Ball JA, Dawson AM. Microscopic colitis-a cause of chronic watery diarrhoea. Br Med J (Clin Res Ed). 1982; 285:1601–1604.

Kubinova L. Advantages of stereological methods in biomedicine. Efficiently obtaining unbiased estimates of geometrical characteristics for 3-D structures. IEEE engineering in medicine and biology magazine : the quarterly magazine of the Engineering in Medicine & Biology Society. 1998; 17:110–115.

Kubinova L, Janacek J. Estimating surface area by the isotropic fakir method from thick slices cut in an arbitrary direction. Journal of microscopy. 1998; 191:201–211. [PubMed: 9767484]

Kubinova L, Janacek J. Confocal microscopy and stereology: estimating volume, number, surface area and length by virtual test probes applied to three-dimensional images. Microscopy research and technique. 2001; 53:425–435. [PubMed: 11525261]

Kubinova L, Janacek J, Ribaric S, Cebasek V, Erzen I. Three-dimensional study of the capillary supply of skeletal muscle fibres using confocal microscopy. J Muscle Res Cell M. 2001; 22:217–227.

Kubinova L, Mao X, Janacek J, Archambeau JO. Stereology techniques in radiation biology. Radiation research. 2003; 160:110–119. [PubMed: 12816530]

Larsen JO. Stereology of nerve cross sections. Journal of neuroscience methods. 1998; 85:107–118. [PubMed: 9874147]

Limsui D, Pardi DS, Smyrk TC, Abraham SC, Lewis JT, Sanderson SO, Kammer PP, Dierkhising RA, Zinsmeister AR. Observer variability in the histologic diagnosis of microscopic colitis. Inflammatory bowel diseases. 2009; 15:35–38. [PubMed: 18623168]

Lokkegaard A, Nyengaard JR, West MJ. Stereological estimates of number and length of capillaries in subdivisions of the human hippocampal region. Hippocampus. 2001; 11:726–740. [PubMed: 11811667]

Luciw PA, Oslund KL, Yang X-w, Adamson L, Ravindran R, Canfield DR, Tarara R, Hirst L, Christensen M, Lerche NW, Offenstein H, Lewinsohn D, Ventimiglia F, Brignolo L, Wisner ER, Hyde DM. Stereological analysis of bacterial load and lung lesions in nonhuman primates (rhesus macaques) experimentally infected with Mycobacterium tuberculosis. American Journal of Physiology - Lung Cellular and Molecular Physiology. 2011; 301:L731–L738. [PubMed: 21873450]

Mayhew TM. A Review of Recent Advances in Stereology for Quantifying Neural Structure. J Neurocytol. 1992; 21:313–328. [PubMed: 1607876]

McKenna P, Hoffmann C, Minkah N, Aye PP, Lackner A, Liu Z, Lozupone CA, Hamady M, Knight R, Bushman FD. The macaque gut microbiome in health, lentiviral infection, and chronic enterocolitis. PLoS pathogens. 2008; 4:e20. [PubMed: 18248093]

Nyengaard JR, Gundersen HJG. The Isector - a Simple and Direct Method for Generating Isotropic, Uniform Random Sections from Small Specimens. J Microsc-Oxford. 1992; 165:427–431.

Olesen M, Eriksson S, Bohr J, Jarnerot G, Tysk C. Microscopic colitis: a common diarrhoeal disease. An epidemiological study in Orebro, Sweden, 1993–1998. Gut. 2004; 53:346–350. [PubMed: 14960513]

Pardi DS. Microscopic colitis: an update. Inflammatory bowel diseases. 2004; 10:860–870. [PubMed: 15626904]

Pardi DS, Loftus EV, Smyrk TC, Kammer PP, Tremaine WJ, Schleck CD, Harmsen WS, Zinsmeister AR, Melton LJ, Sandborn WJ. The epidemiology of microscopic colitis: a population based study in Olmsted County, Minnesota. Gut. 2007; 56:504–508. [PubMed: 17135309]

Pardi DS, Smyrk TC, Tremaine WJ, Sandborn WJ. Microscopic colitis: A review. American Journal of Gastroenterology. 2002; 97:794–802. [PubMed: 12003412]

Sestak K, Merritt CK, Borda J, Saylor E, Schwamberger SR, Cogswell F, Didier ES, Didier PJ, Plauche G, Bohm RP, Aye PP, Alexa P, Ward RL, Lackner AA. Infectious agent and immune response characteristics of chronic enterocolitis in captive rhesus macaques. Infection and immunity. 2003; 71:4079–4086. [PubMed: 12819098]

Shah RJ, Fenoglio-Preiser C, Bleau BL, Giannella RA. Usefulness of colonoscopy with biopsy in the evaluation of patients with chronic diarrhea. The American journal of gastroenterology. 2001; 96:1091–1095. [PubMed: 11316152]

Tangri V, Chande N. Microscopic colitis: an update. Journal of clinical gastroenterology. 2009; 43:293–296. [PubMed: 19169149]

Teigler JE, Iampietro MJ, Barouch DH. Vaccination with Adenovirus Serotypes 35, 26, and 48 Elicits Greater Innate Cytokine Responses Than Adenovirus Serotype 5 in Rhesus Monkeys. Journal of virology. 2012

Uranova NA, Vostrikov VM, Orlovskaya DD, Rachmanova VI. Oligodendroglial density in the prefrontal cortex in schizophrenia and mood disorders: a study from the Stanley Neuropathology Consortium. Schizophr Res. 2004; 67:269–275. [PubMed: 14984887]

Warren BF, Edwards CM, Travis SP. 'Microscopic colitis': classification and terminology. Histopathology. 2002; 40:374–376. [PubMed: 11943023]

Weibel ER, Hsia CCW, Ochs M. How much is there really? Why stereology is essential in lung morphometry. J Appl Physiol. 2007; 102:459–467. [PubMed: 16973815]

West MJ. Isotropy, iSectors, and vertical sections in stereology. Cold Spring Harbor protocols 2013. 2013

West MJ, Gundersen HJG. Unbiased Stereological Estimation of the Number of Neurons in the Human Hippocampus. J Comp Neurol. 1990; 296:1–22. [PubMed: 2358525]

West MJ, Slomianka L, Gundersen HJ. Unbiased stereological estimation of the total number of neurons in the subdivisions of the rat hippocampus using the optical fractionator. The Anatomical record. 1991; 231:482–497. [PubMed: 1793176]

Wilk JL, Maginnis GM, Coleman K, Lewis A, Ogden B. Evaluation of the use of coconut to treat chronic diarrhea in rhesus macaques (Macaca mulatta) . Journal of medical primatology. 2008; 37:271–276. [PubMed: 19017194]

Wreford NG. Theory and practice of stereological techniques applied to the estimation of cell number and nuclear volume in the testis. Microscopy research and technique. 1995; 32:423–436. [PubMed: 8563041]

Yen EF, Pardi DS. Review article: Microscopic colitis--lymphocytic, collagenous and 'mast cell' colitis. Alimentary pharmacology & therapeutics. 2011; 34:21–32. [PubMed: 21545473]

Zippi M, Marcheggiano A, Crispino P, Occhigrossi G, Severi C. Microscopic colitis: a concise review. Clin Ter. 2010; 161:385–390. [PubMed: 20931164]

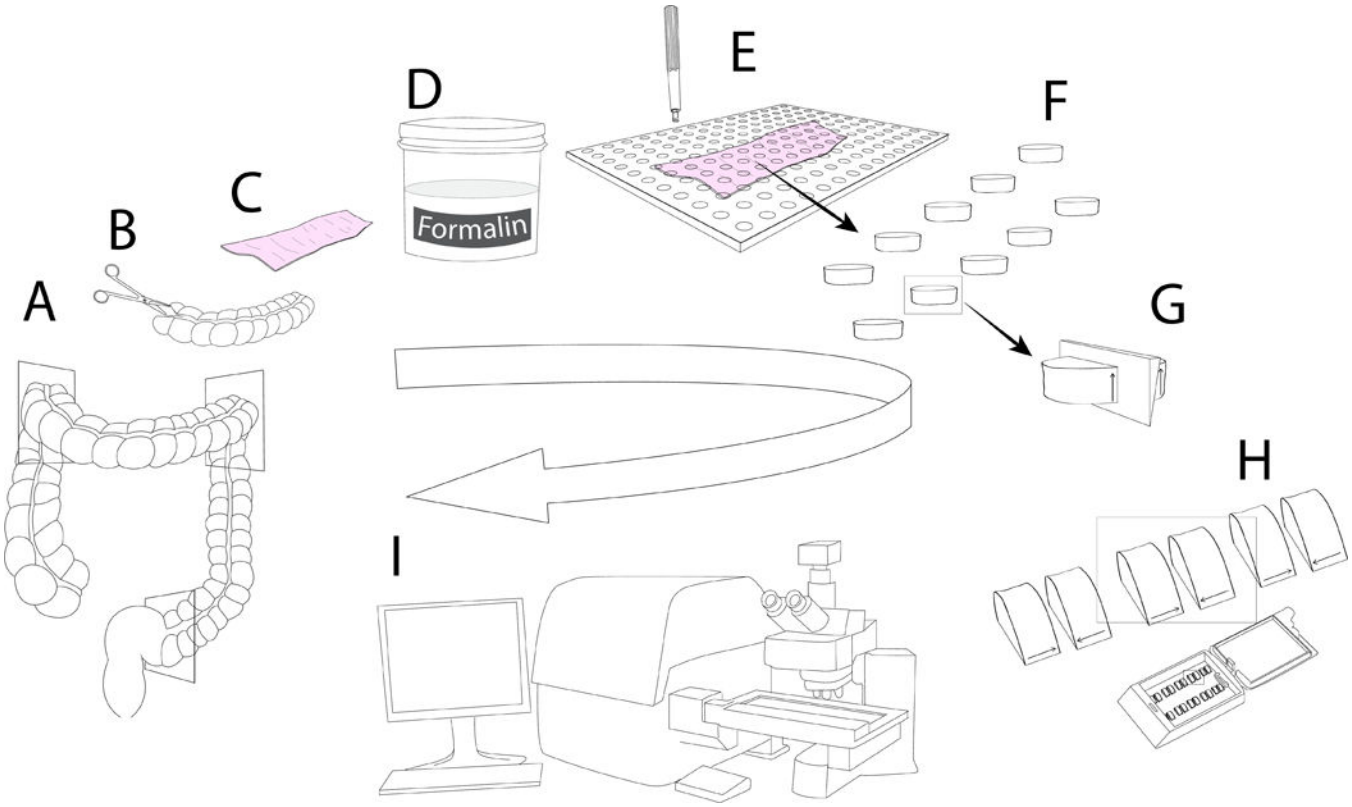

Figure 1.

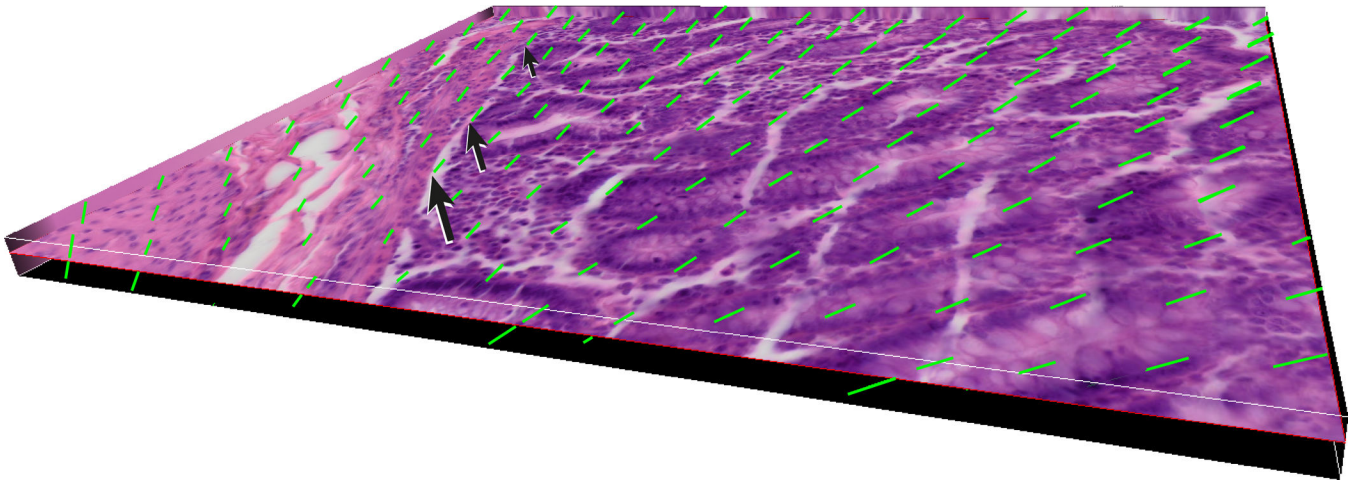

Figure 2.

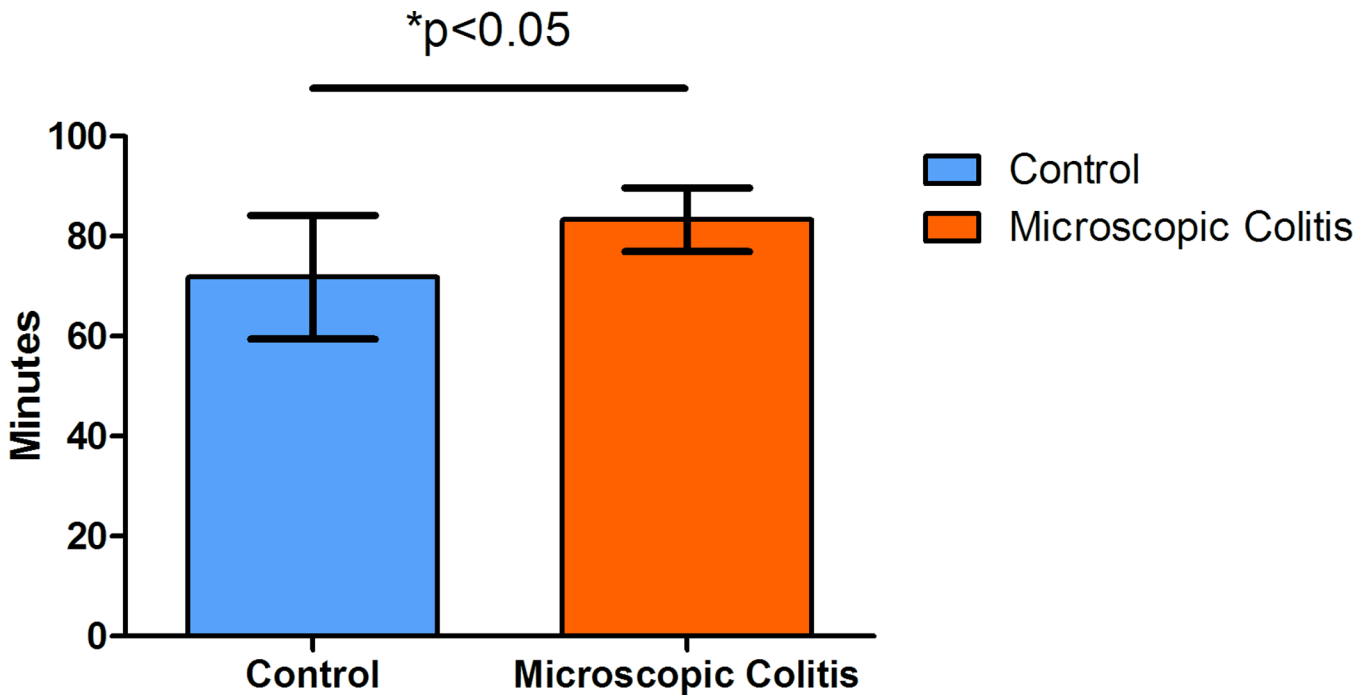

Figure 3.

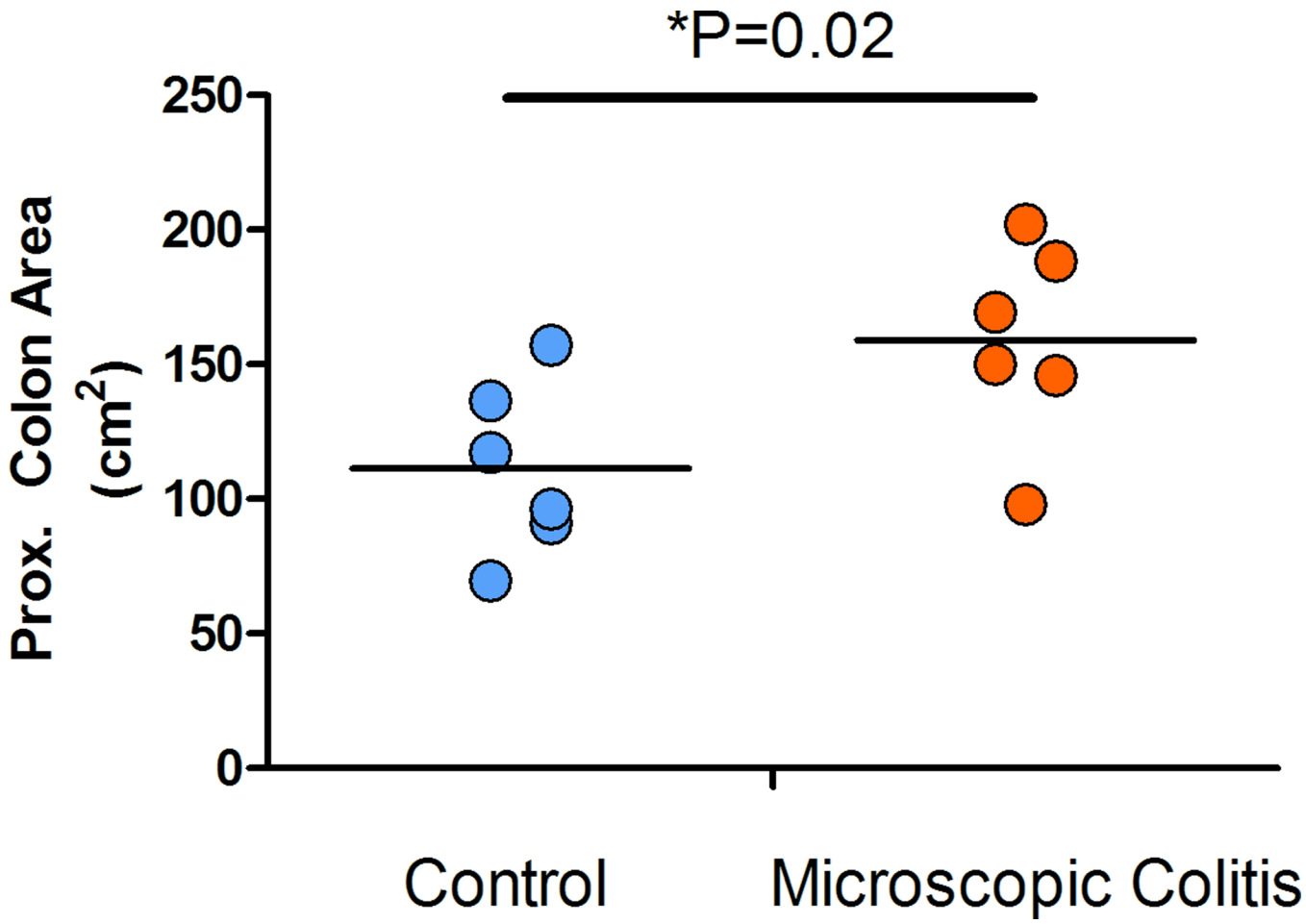

Figure 4.

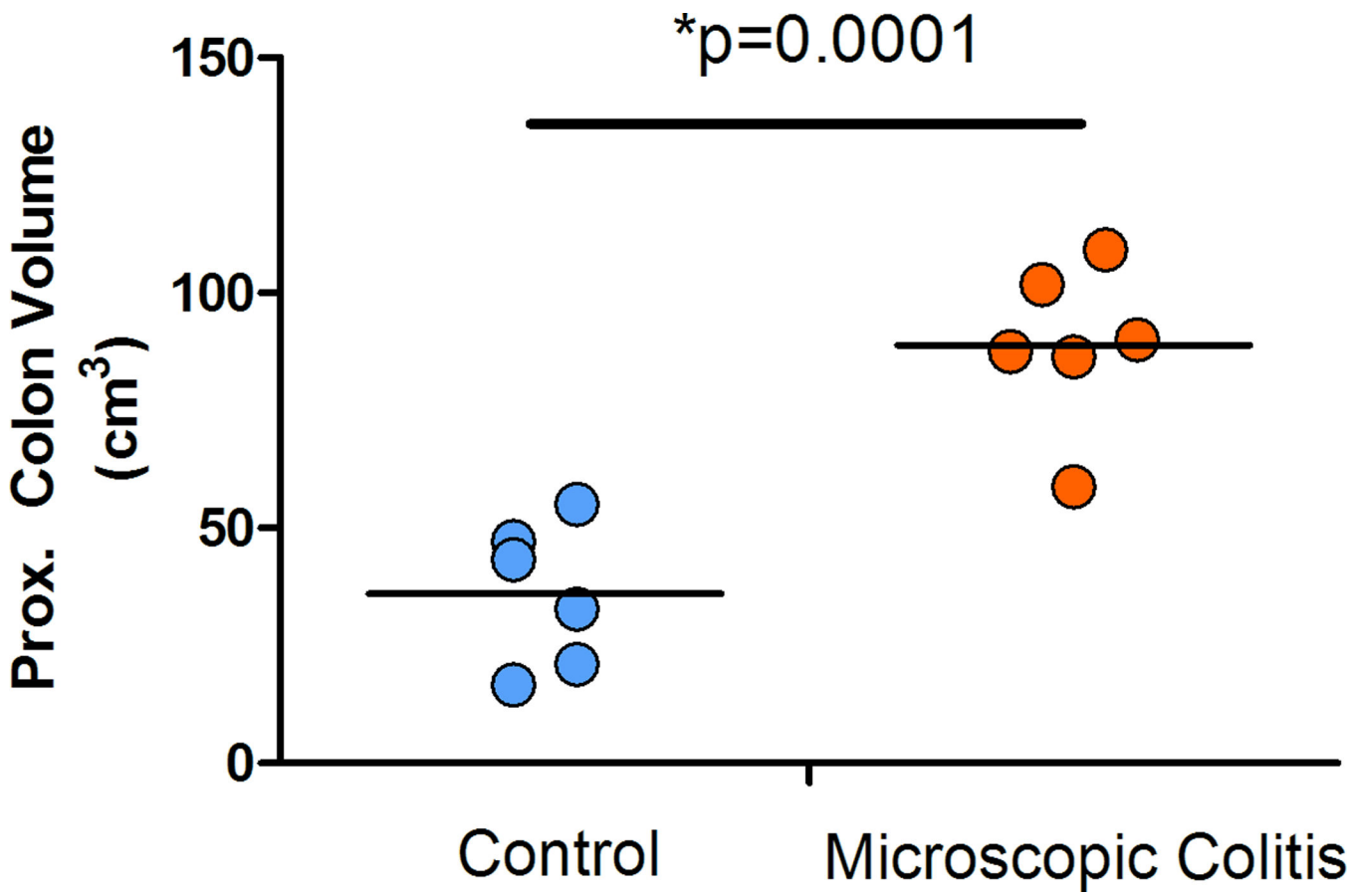

Figure 5.

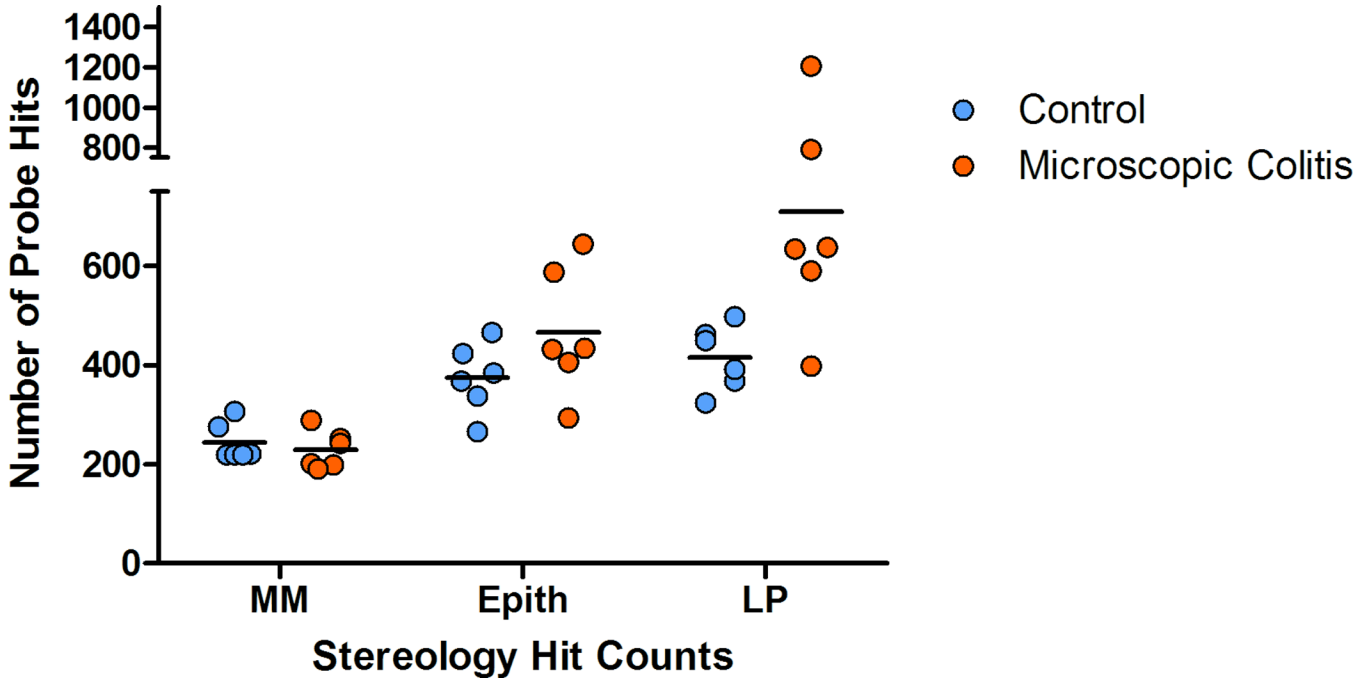

Figure 6.

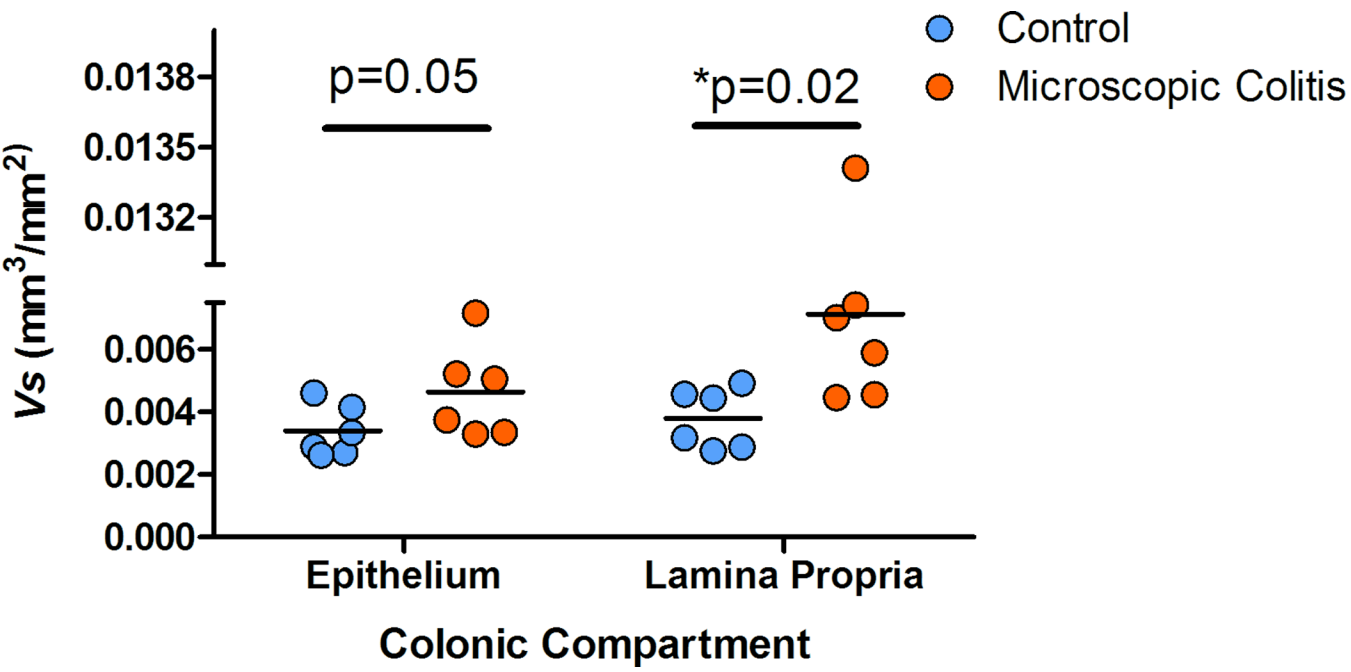

Figure 7.

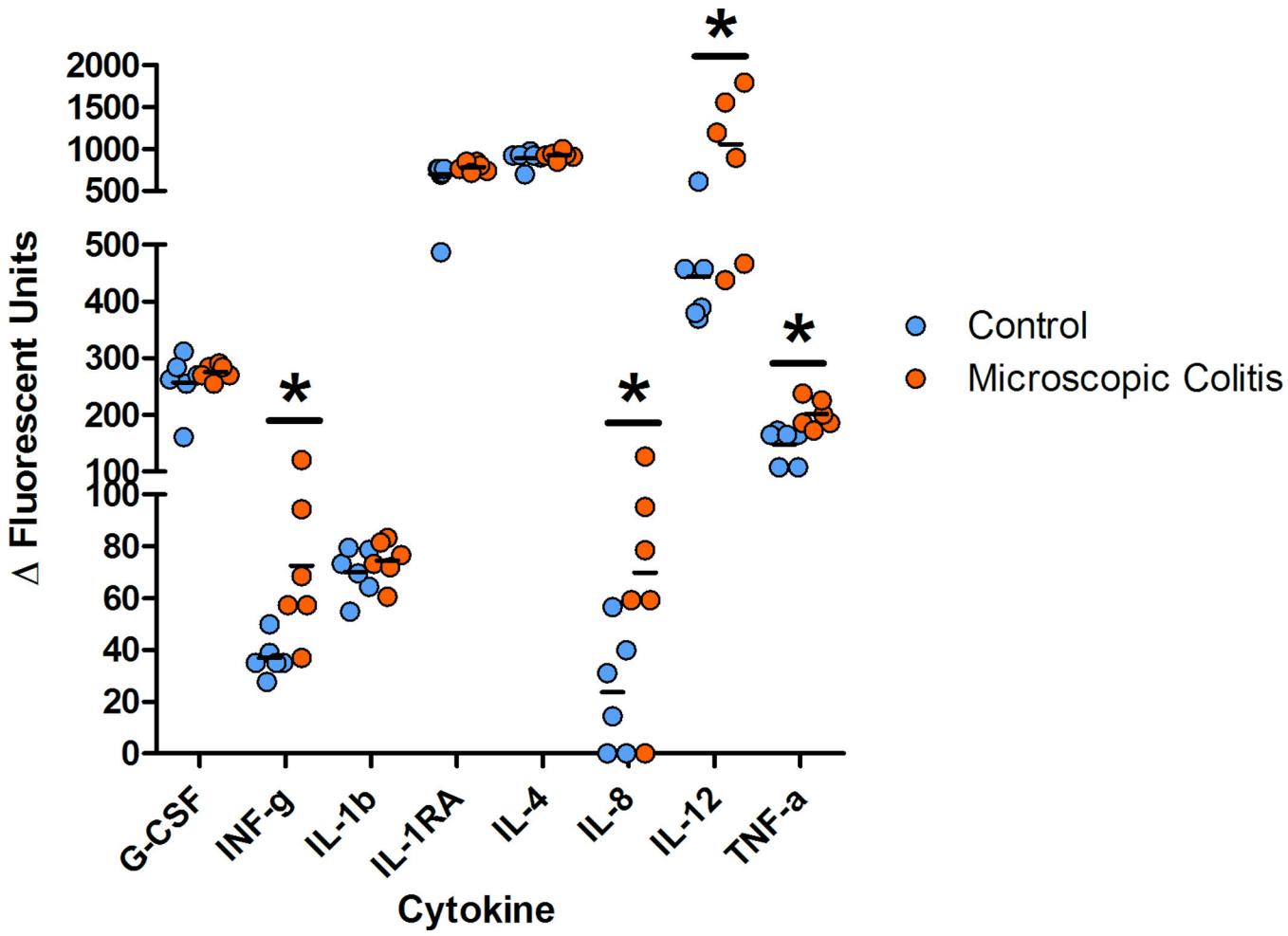

Figure 8.

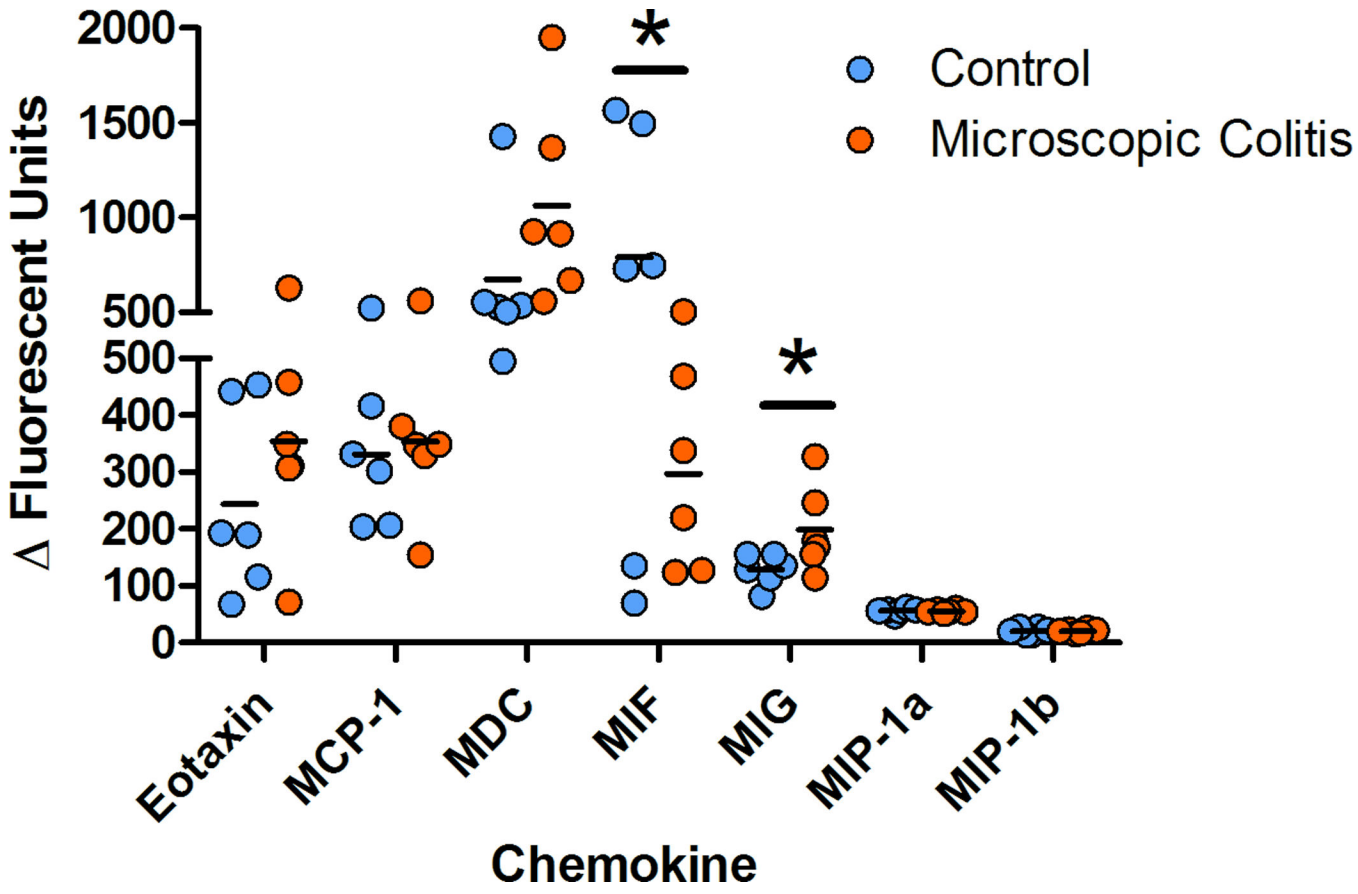

Figure 9.

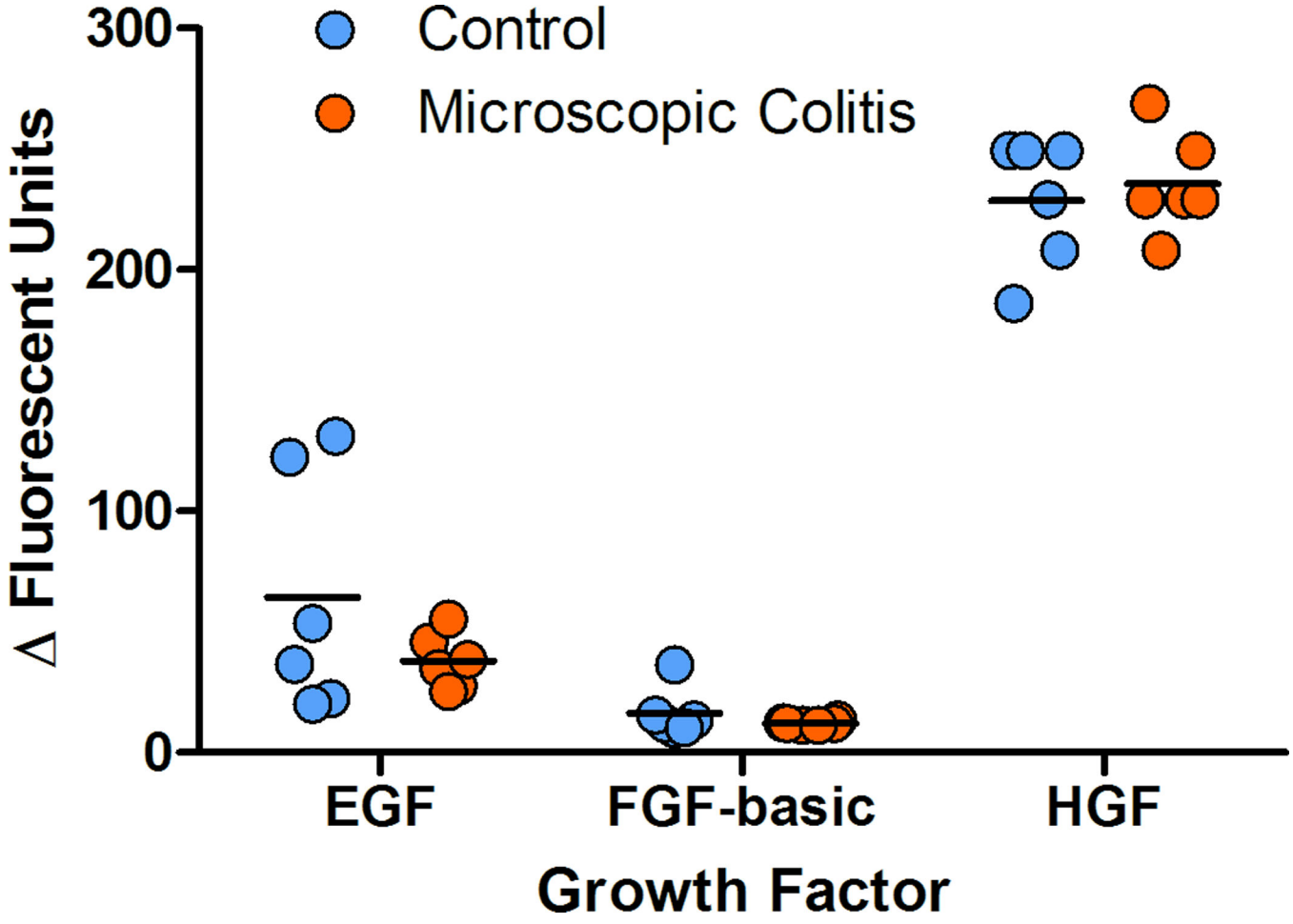

Figure 10.

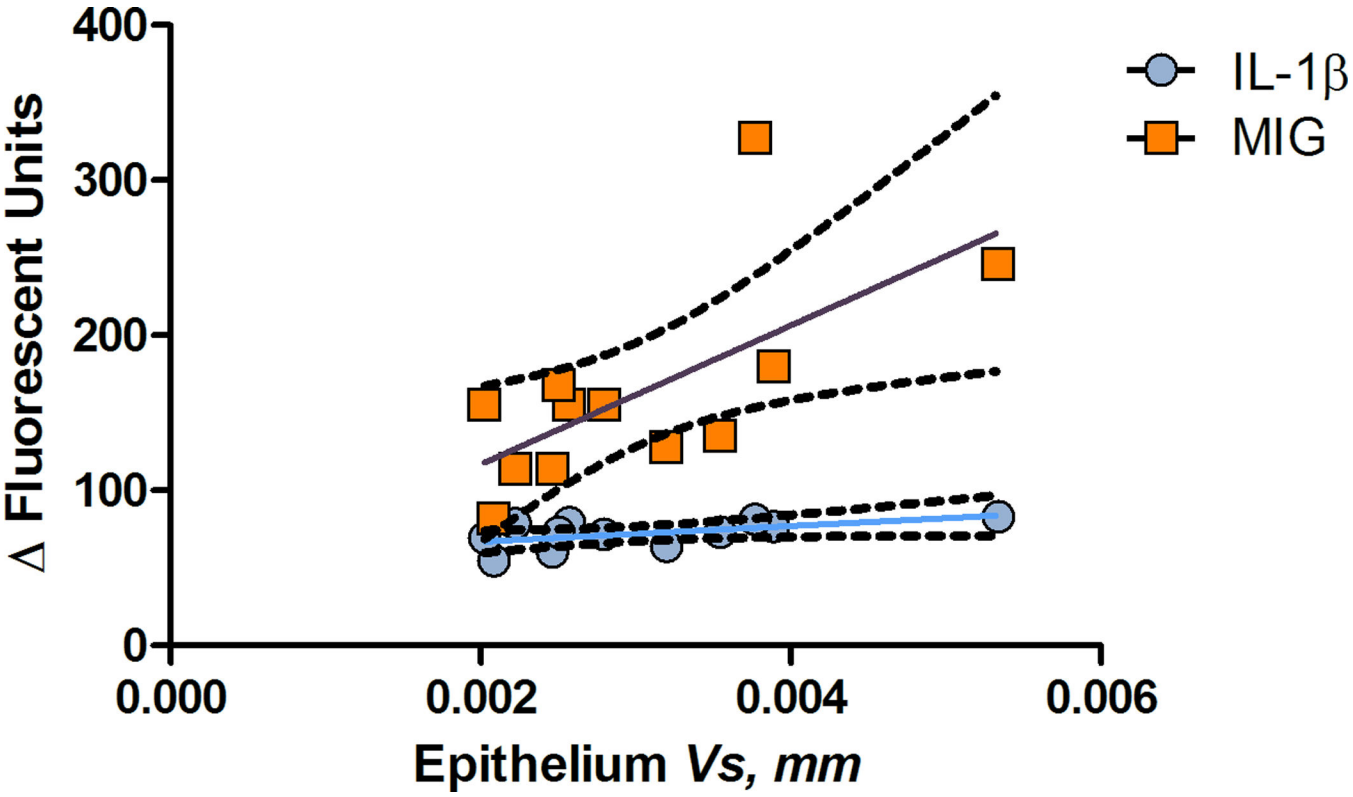

Figure 11.

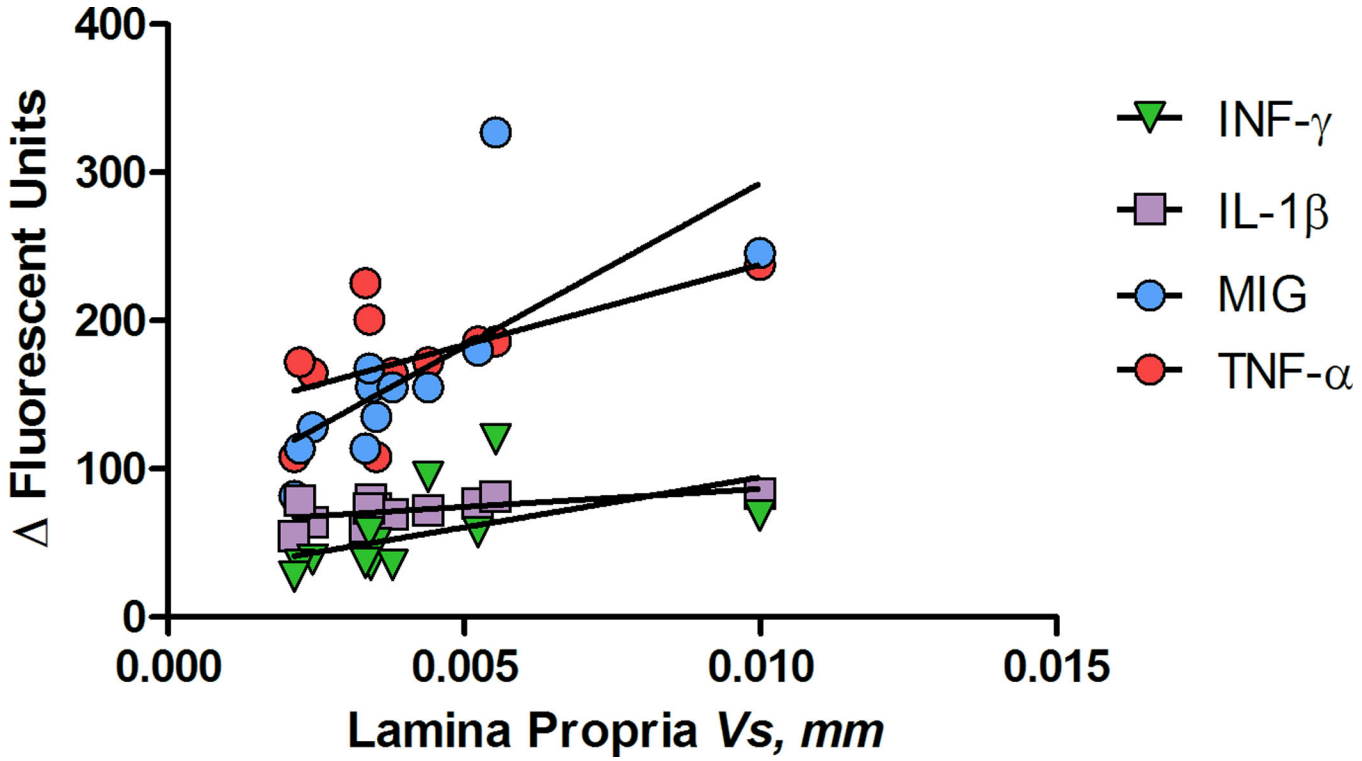

Figure 12.

Table 1

Demographic information of the monkeys assigned to the study

Animal ID	Group	Necropsy Reason	Age at Sampling
CNTRL1	Control	Trauma	3 yrs 10 mos
CNTRL2	Control	Arthritis	3 yrs 2 mos
CNTRL3	Control	Trauma	3 yrs 9 mos
CNTRL4	Control	Trauma	3 yrs 10 mos
CNTRL5	Control	Arthritis	3 yrs 2 mos
CNTRL6	Control	Arthritis	2 yrs 1 mos
MC1	ICD	Chronic Diarrhea	4 yrs
MC2	ICD	Chronic Diarrhea	3 yrs 2 mos
MC3	ICD	Chronic Diarrhea	2 yrs 10 mos
MC4	ICD	Chronic Diarrhea	2 yrs 5 mos
MC5	ICD	Chronic Diarrhea	3 yrs 2 mos
MC6	ICD	Chronic Diarrhea	2 yrs 9 mos

Table 2

The link between the probe dimension and the dimension of the structure of interest

Dimension of the feature of interest	Probe Type
Volume (3D)	Point (0D)
Surface (2D)	Linear (1D)
Length (1D)	Surface (2D)
Number (0D)	Volume (3D)

Table 3

The R square values (square of the sample correlation coefficient) were calculated to describe the relative amount of variance of the *Vs* differences for colonic compartments explained for by the serum analytes

		INF-γ	IL-1β	IL-1RA	IL-8	IL-12	MIF	MIG	TNF-α
Epithelium *Vs*	Pearson r	0.495	0.563	0.216	0.348	0.279	−0.114	0.659	0.398
	95% confidence interval	(−0.111 – 0.832)	(−0.0156 – 0.859)	(−0.409 – 0.703)	(−0.283 – 0.768)	(−0.351 – 0.735)	(−0.646 – 0.492)	(0.136 – 0.894)	(−0.228 – 0.791)
	R square	0.245	0.317	0.0467	0.121	0.0779	0.0131	0.434	0.159
	p-value	0.0511	*0.0282	0.2499	0.134	0.1899	0.3618	*0.0099	0.0998
Lamina Propria *Vs*	Pearson r	0.519	0.597	−0.0214	0.496	0.232	−0.243	0.716	0.594
	95% confidence interval	(−0.0790 – 0.842)	(0.0345 – 0.872)	(−0.588 – 0.559)	(−0.110 – 0.833)	(−0.394 – 0.711)	(−0.717 – 0.384)	(0.241 – 0.914)	(0.0310 – 0.871)
	R square	0.269	0.356	0.000459	0.246	0.0539	0.0593	0.512	0.353
	p-value	*0.0421	*0.0203	0.4737	0.0507	0.2339	0.2229	*0.0044	*0.0208